Organic-Inorganic Nano-Composite of PMMA-Forsterite Doped with Eu^{+3}

Dong Gon Park,[*] Jin Kang, and Hea Young Kwon

Department of Chemistry, Sookmyung Women's University, Seoul 140-742, Korea
Received October 9, 1999

Drying-step in sol-gel processing was bypassed by exchanging alcoholic solvent in forsterite alcogel directly with MMA. By *in-situ* polymerization of the MMA, organic-inorganic nano-composite of PMMA-forsterite was prepared. As porous nature of inorganic networks in the gel was preserved and fixated in the composite, spherical morphology of PMMA was resulted. The PMMA-forsterite composite was optically transparent, machinable, mechanically sustainable, and thermally more stable than pristine PMMA. When doped with Eu^{+3}, inorganic moiety in the composite provided site environment that is very different from that in pristine PMMA. Prominent $^5D_o \rightarrow {}^7F_o$ transition at 578 nm, broken degeneracy in $^5D_o \rightarrow {}^7F_1$ and $^5D_o \rightarrow {}^7F_2$ transitions suggested that Eu^{+3} was exclusively doped in the inorganic moiety of the composite, which had lower symmetry than the organic counterpart.

Introduction

Sol-gel reaction is very versatile synthetic method to prepare solid products in various different exotic forms.[1,2] Solid products can be obtained as thin films, uniform sized submicron particles, monolithic bulks, or even as fibers. Recent addition to the products is the hybrid materials, which are being called the organic-inorganic composites. This new composite material is usually named as a CERAMER (CERAmic + polyMER)[3] or as an ORMOCER (Organically Modified CERamic).[4]

Many different approaches have been reported in getting the CERAMERs. Organofunctional metal alkoxide was introduced as a bridging component between inorganic and organic moieties in the composite.[5-7] Useful products, such as optical films, protective films, or contact lenses, were obtained by this synthetic approach. The composite was also obtained by carrying out sol-gel reaction directly in polymeric media.[8] But, this method often suffers from severe phase separation. The composite was also obtained by synchronously carrying out polymerization of both inorganic and organic moieties at the same time.[9-11] But, careful design of the reactants is required and reaction conditions are very restricted.

Novak and coworkers synthesized the composite by infiltrating various organic polymers into the aerogel of silica obtained by the hypercritical drying.[12] It was observed that chemical bonding between inorganic and organic moieties was essential to get the composite. Without having such bonding site, poly(methyl methacrylate) (PMMA) leached out from the aerogel, failing the synthesis of the composite. Therefore, the composite with PMMA could not be made by this method.

The composite was also made simply by carrying out polymerization of organic constituents in a monolithic xerogel.[13,14] As an example, a monolithic xerogel of silica was dipped into methyl methacrylate (MMA), then MMA was polymerized into poly(methyl methacrylate) (PMMA). This method seems to be very useful in getting organic-inorganic composite of various applicable materials. But, slow careful

drying of alcogel during extended time is required to get the monolithic xerogel in decent quality.[14] More over, obtaining large crack-free monolithic xerogel is very difficult. When the chemical composition of the xerogel exceeds two, such as in forsterite (Mg$_2$SiO$_4$/magnesium and silicon), getting it in decent quality is practically impossible. Therefore, without solving the problems that are originated from the drying step of the sol-gel synthesis, no further application of this methodogy is expected.

In a previous communication,[15] we reported a new synthetic strategy to prepare an organic-inorganic nano-composite by skipping over the problematic drying step of the sol-gel process. Key step in the strategy was exchanging alcoholic solvent in the alcogel, directly with organic monomer. Thereby, the drying step was bypassed. Bypassing the drying step eliminated all those problematic phenomena, such as shrinkage, cracks, or warping. Because no shrinkage was involved, the inorganic moiety in the alcogel was preserved into the composite, thereby making it possible to get a nano-composite. In this study, we report further details on the preparation of the organic-inorganic nano-composite of the PMMA-forsterite, which was doped with an optically active component, Eu^{+3}.

Experimental Section

Synthesis of the organic-inorganic nano-composite of the PMMA-forsterite was schematically summarized in Figure 1. Forsterite (Mg$_2$SiO$_4$) alcogel was synthesized by the H$_2$O$_2$-assisted sol-gel method under argon by using Schlenk line.[16] The alcogel was aged for 3 days into thicker one, while it was mechanically stirred under argon. At the end of the aging, the gel was mixed with same volume of toluene, and tetrabutyl ammonium hydroxide (0.025 g/100 mL toluene). In ambient air, the gel was stirred and heated at 55-60 °C for 7 hours. Inorganic component in the gel was separated from solvent by centrifuging the gel at 3000 rpm for 60 min. Volume of the gel was decreased to 1/3 of the original after the centrifugation. Raising centrifuging time did not shrink
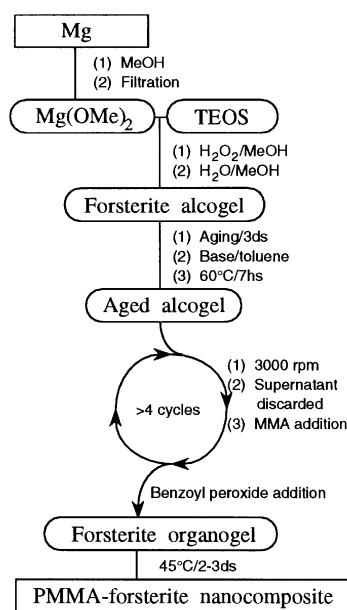
Figure 1. Schematic description of the synthesis of nano-composite of the PMMA-forsterite. The forsterite alcogel was prepared by the H_2O_2-assisted sol-gel method.[16]

the volume much further. Supernatant (solvent) over the collection (densified gel) was decant and discarded. In order to check the loss of the inorganic component, some supernatant was dried in a separate vessel to see if there were any remnants. No loss was observed. Methyl methacrylate (MMA), about 4 times (volume-wise) that of the densified gel, was then added to the collection, and the mixture was well stirred back into a diluted gel. By going through the centrifugation-redilution several times (usually 4 rounds) in the same manner, content of MMA in the gel was raised above >99%. The gel which was produced by exchanging alcohol with MMA was designated as an 'organogel'.[15] In the last round of the centrifugation, benzyl peroxide was added as an initiator for radical polymerization of MMA. After the last round of the centrifugation, supernatant over the collection was remained over the densified 'organogel'. Because there was decrease of the volume (about 1/10 volume-wise) while MMA was polymerized into PMMA, the supernatant MMA acted as a capping over the gel. Without the capping, the shape of the composite was severely deformed during polymerization of MMA.

Radical polymerization of MMA in the 'organogel' was carried out by incubating the gel in an oven at 45 °C for 2-3 days. Final product of the PMMA-forsterite nano-composite was obtained as a cylindrical bar (2 cm dia. × 2-4 cm long), since cylindrical mold was used. The bar was consisted of two parts: the composite of the PMMA-forsterite on the bottom, and the sole PMMA (from the capping) on top of the composite. The bar was sawed into several wafers whose surface was polished.

Transmittance through the wafers was measured by obtaining UV-vis spectrum with Shimadzu UV-1601PC spectrophotometer. Inorganic content of the wafer was calculated from the content of organic counterpart measured by elemen-

tal analysis. The calculation was also propped up by measuring metal content by ICP/MS. Morphology of the broken surface (cross-section of the wafer) of the composite was measured by atomic forced microscopy (AFM) with AP-0100 Park Scientific Instrument. The broken surface was treated in sonicated bath for a few minutes before AFM measurement. The broken surface was also etched by dipping a piece of the wafer in diluted aqueous solution of nitric acid. Etched surface was washed by sonication in distilled water before AFM measurement. Concentration of the acid solution was stepwise increased from 0.1 N to 1.0 N.
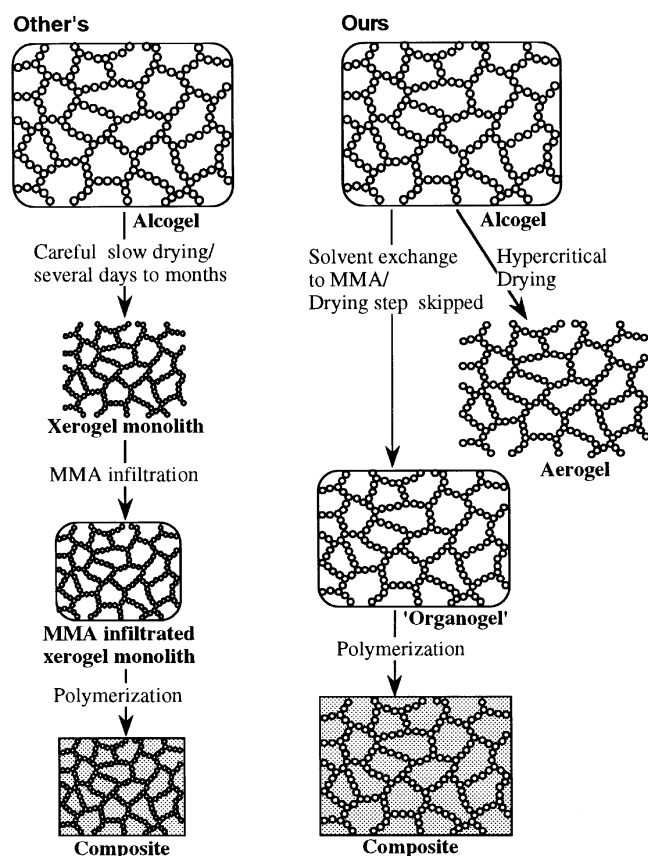
Simultaneous differential thermal and thermogravimetric analysis (DT/TGA) was carried out by using Seiko TG/DTA-320. Heating rate was 3 °C/min, and the rate of air flow over the sample was 30 mL/min. For carrying out gel permeable chromatography (GPC), the composite was dissolved in tetrahydrofuran (THF), and filtered through 0.45 μm syringe filter, in order to separate the inorganic moiety from PMMA. Filtration was carried out several times to get rid of the inorganic precipitates from the solution. Surface hardness was measured by diamond indentation. Mechanical strength as a bulk was measured by three point bending test. The size of the sample was 20 × 1 × 4 mm^3.

Optically active probe, Eu^{+3}, was doped to the forsterite alcogel in the same manner used in preparing the chromium-doped forsterite.[16] Eu^{+3} was doped into the alcogel by adding 1.15 g $Eu(NO_3)_3$ dissolved in 100 mL methanol (MeOH) into the reaction mixture of 2.55 g $Mg(OMe)_2$ and 10.42 g tetraethyl orthosilicate (TEOS) in 200 mL MeOH. Eu^{+3} dopant to silicon mole ratio was 0.05. Fluorescence spectra were taken from solid samples (in form of polished wafers) doped with the probe, by using SPEX fluorelog-T2. Excitation wavelength was 393 nm.

Forsterite aerogel was synthesized by hypercritically removing alcoholic solvent from the forsterite alcogel, at 265 °C and 1,000 psi by using pressurized reaction vessel, purchased from Parr. The isothem of nitrogen adsorption-desorption was obtained by using Micromeritics ASAP 2400.

Results and Discussion

Major difference between conventional way of getting a composite from a xerogel and our way of bypassing the drying step was conceptually compared in Scheme 1. Main target of our synthetic scheme was to bypass the problematic drying step in getting the organic-inorganic composite. As was pointed out in previous communication,[15] drying step was skipped over by exchanging alcohol directly with methylmethacrylate (MMA), without going through unnecessary step of getting the xerogel. Solvent exchange was carried out by washing the forsterite alcogel with MMA. Centrifugal force was applied to collect only the inorganic moiety of the gel. Carrying out several rounds of centrifugation-redilution gradually raised the content of MMA. Thereby, an 'organogel' of forsterite was obtained, instead of the xerogel.[15] In order to collect the inorganic moiety without loss, forsterite

Other's

Ours

Scheme 1

Figure 2. UV-vis spectra taken from pristine PMMA (A), and from two different kinds of the PMMA-forsterite composite (B and C). The composite (B) was prepared from transparent alcogel, whereas (C) was from turbid one. Weight percent of the inorganic moiety was same for both samples.

alcogel had to be aged for several days. The gel was also sta-bilized in toluene with addition of base. It was presumed that the inorganic moiety was densified by condensation reaction during the process. After alcohol in the gel was thoroughly replaced with MMA, it was radically polymerized by using peroxide initiator. By thermal initiation, MMA in the 'organ-ogel' was *in-situ* polymerized into poly(methyl methacry-late) (PMMA). Thereby, the organic-inorganic composite of PMMA-forsterite was obtained.

Viscous forsterite alcogel obtained by the H_2O_2-assisted sol-gel method was transparent and clear with a tint of hazi-ness, suggesting the size of gel particle was sub-micron. The composite of PMMA-forsterite was also transparent and clear with a tint of haziness. When the forsterite alcogel was turbid, mostly because too much aging was carried out, the composite also got turbid by scattering. UV-vis spectra in Figure 2 showed that optical transparency of the composite was largely dependent on quality of the forsterite alcogel. Spectrum A was for the composite made out of a clear alco-gel. Transparency in visible region reached near to that of pristine PMMA. Compared to the pristine PMMA (spectrum A), transmittance was maintained at 98%. Whereas transmit-tance in visible range was decreased, that in ultraviolet was slightly increased. This observation was similar to the one made by others on the organic-inorganic composite of silica-PMMA.[14] It was observed that transmittance by silica in ultraviolet region was higher than that of PMMA. The spec-trum B and C showed that optical property of the composite
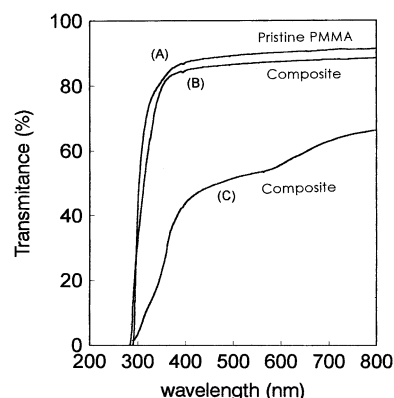
was deteriorated when the alcogel was improperly obtained. When turbidity was developed in the alcogel, the composite made out of the gel exhibited severe scattering in visible range. Scattering occurred most severely below 400 nm. To avoid such deterioration of optical transparency, hydrolysis reaction had to be carried out very slowly, and the gel had to be stabilized in toluene before too much aging was pro-gressed.

In preparing the inorganic moiety of the composite via the H_2O_2-assisted sol-gel method, gelation was carried out in methanol, and water to methoxy ratio (r = H_2O/-OMe) was 1, which was considered to be in lower end.[17] *In-situ* gener-ated peroxide of magnesium, -Mg-OOH, acted as catalyst for hydrolysis.[18] Therefore, no acid or base was added dur-ing hydrolysis and condensation. These synthetic variables established condition of particle growth in diffusion-limited regime.[19] In such condition, particles in mass fractal were generated, which in turn should generate inorganic networks with much void in it. Such structure with severe networking and large void doesn't have enough mechanical strength to sustain itself during removal of solvent in the void. There-fore, it was very hard to obtain monolithic xerogel of forster-ite in decent quality. As drying step was bypassed in pre-paring the composite, such fractal structure was preserved intact, and was fixated into a matrix of PMMA in the com-posite.

In order to get an information on morphology of the com-posite, the forsterite aerogel was obtained by hypercritically removing alcohol solvent, without disturbing the network structure.[20] Because capillary stress by alcohol was elimi-nated in its critical state, destruction of the network structure was presumed to be not significant.[21] PMMA should fill the void of the networks generated by inorganic moiety of the gel. Therefore, it was suggested that the characteristics of the void in the forsterite aerogel appropriately described the PMMA moiety in the composite.

The forsterite aerogel obtained by the hypercritical drying at 265 °C and 1000 psi had very high BET surface area of 806 m^2/g. Translucent monolithic chunk could be obtained,
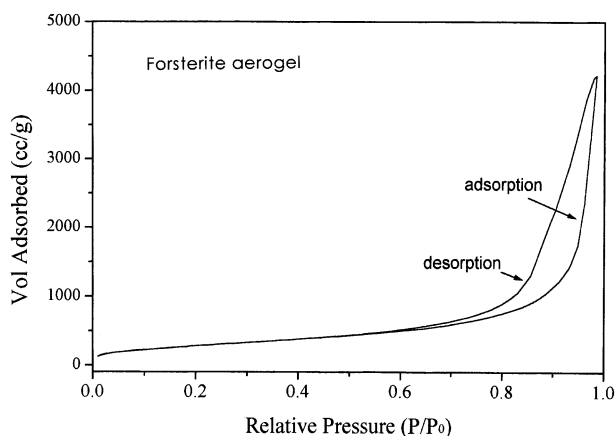
Figure 3. Isotherm curves of nitrogen adsorption and desorption measured on forsterite aerogel, which was prepared by hypercritical drying of the forsterite alcogel.
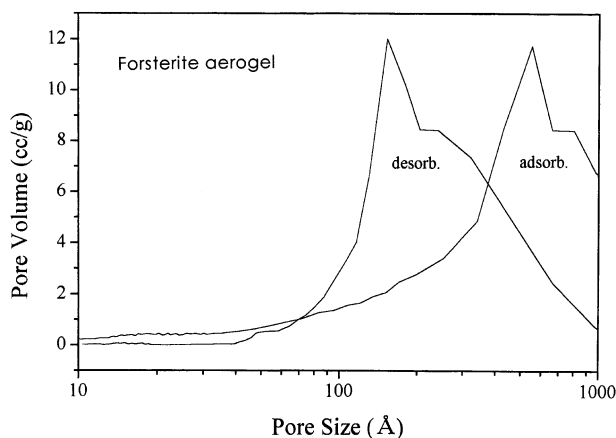

Figure 4. Size distribution of pores in the forsterite aerogel that was calculated from the isotherm in figure 3.

Broken surface of PMMA

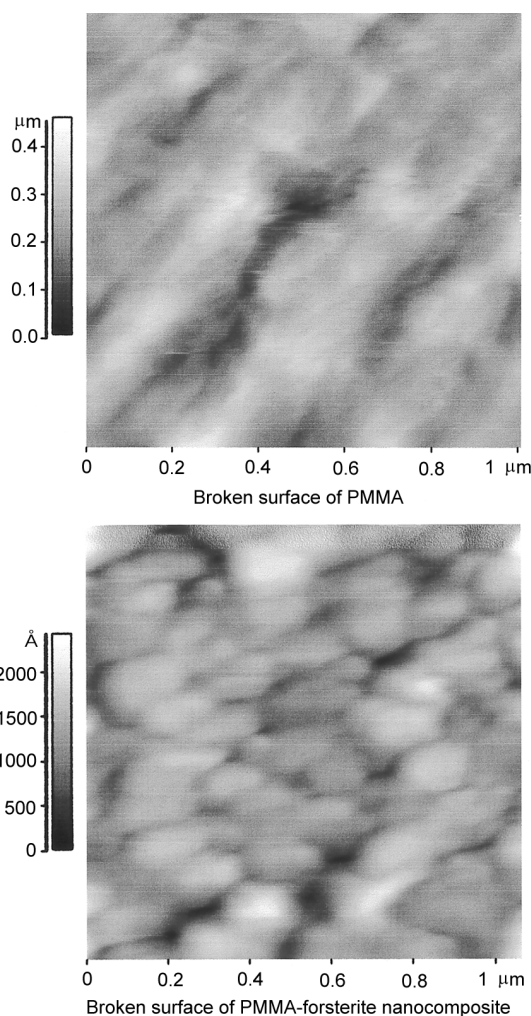Broken surface of PMMA-forsterite nanocomposite

Figure 5. The texture of broken cross-section of pristine PMMA (A), and of the composite of the PMMA-forsterite (B), that was measured by atomic forced microscope.

but it readily disintegrated into fluffy powder just by pressing lightly between fingers. Figure 3 and 4 showed characteristics of the void in the forsterite aerogel, which were measured by adsorption-desorption of nitrogen on the surface of the aerogel. Isotherm of the nitrogen adsorption-desorption was type IV of mesoporous solid.[22] The hysteresis of the isotherm was near to type H2.[23] This observation indicated that the void in the aerogel was consisted mostly of mesopores in nearly ink-bottled shape. The pore distribution in Figure 4 verified that dimension of neck of the bottle was around 100 nm, and that in the middle was around 400 nm. Size distribution of the pores was broad, which was typical for the fractal structure. On the contrary, the isotherm obtained from the composite was type II with no hysteresis, that was for a nonporous solid. Surface area measured on pulverized powder of the composite was only 5-6 m^2/g. Therefore, polymerization of MMA inside the void was considered to leave no empty space.

Assuming the void was all filled with PMMA, theoretical weight of the inorganic moiety in the composite was calculated to be 11%. Considering some shrinkage is unavoidable even during hypercritical drying,[24] actual weight of the inor-

ganic moiety in the composite would be less than 11%. The elemental analyses done by thermal decomposition and by ICP/MS showed that the actual weight of the inorganic moiety in the PMMA-forsterite composite was 8%, which confirmed our anticipation. Therefore, the information on the void of the forsterite aerogel was considered to describe the PMMA moiety of the composite with high similarity.

Pore characteristics of the forsterite aerogel made it possible to conceive the morphology of the composite. PMMA would fill the bottle shaped (spherical) void in the inorganic networks through out the sample. In order to get physical evidence on such morphology of the composite, the broken surface (cross-section) of the composite was observed by AFM, and its image was provided in Figure 5. Compared to pristine PMMA, which showed an irregular pattern (5A), the broken surface of the composite exhibited spherical texture (5B). The size of the spherical structure was 100-300 nm. Illuminating an electron beam on surface of the composite immediately destroyed the structure even at low acceleration voltage. Thereby, microprobe analysis could not be carried out directly on the surface. Instead of directly analyzing the
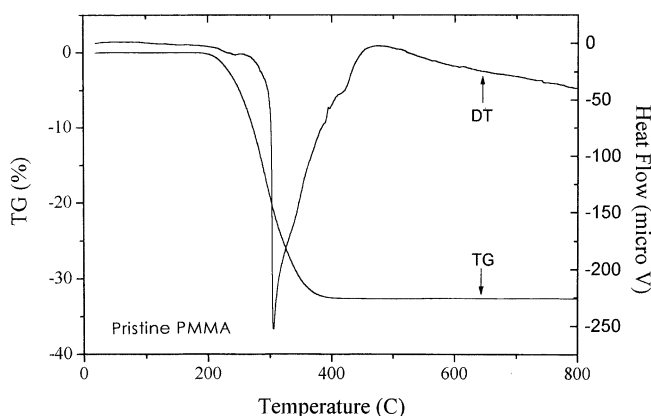
Figure 6. DT and TG curves which were simultaneously obtained on pristine PMMA. Endothermic depolymerization of PMMA started already at 210.
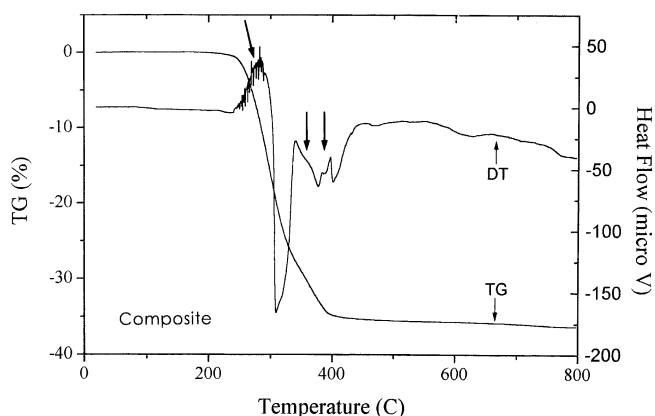

Figure 7. DT and TG curves which were simultanesouly obtained on the composite of the PMMA-forsterite. Prominent exotherms in jagged shape were reproducibly overlaped around 280 °C and 350 °C on the endotherm in the background.

constituent of the structure, the broken surface was etched in 0.5 N HNO_3 aqueous solution, and observed under AFM, which showed the spherical structure was still intact. The spherical structure was destroyed upon raising the concentration of the acid to 1.0 N where surface of pristine PMMA was also destroyed. Considering forsterite aerogel was dissolved already in 0.1 N HNO_3 aqueous solution, it was suggested that the spherical texture be consisted mostly of PMMA. If the texture were the inorganic moiety, it should have been destroyed even in 0.1 N acid solution. Remaining space among those spherical structures constitutes three-dimensional strings of networks, which presumably correspond to the inorganic moiety in the composite.

Thermal property of the PMMA-forsterite composite was measured by thermal analyses, Figure 7, and compared to that of pristine PMMA in Figure 6. Main thermal event was endothermic depolymerization around 300 °C, which accompanied major loss of weight. In pristine PMMA, the weight decrease started around 210 °C, and accompanied a small endotherm. This observation indicated that depolymerization started already at 210 °C for the pristine PMMA. On the contrary, the start of depolymerization was retarded in the composite. Weight decrease started around 260 °C, which was about 50 °C higher than in the pristine PMMA. Therefore, the inorganic network in the composite raised thermal stability of PMMA moiety.

Peculiarly, initial depolymerization of PMMA in the composite, between 260-300 °C, reproducibly accompanied a prominent exotherm in jagged shape. TG trace also had a broad step around 350 °C in the composite. Others also observed such step in TG trace in the organic-inorganic composite of silica-poly(vinyl acetate).[25] This step reproducibly accompanied several small exotherms, which overlaid the jagged pattern on the major endotherm in the background. It was suggested that the exotherms in jagged shape were caused by shrinkage of the inorganic networks. As PMMA matrix was disintegrated by thermal depolymerization, the forsterite network started shrinking. This phenomenon is similar to the shrinkage of the xerogel caused by capillary stress during drying step.[26] In the composite, con-

densation reaction among $\equiv$ Si-OH and −Mg-OH moieties along the adjacent networks would provide further driving force to the shrinkage, which should accompany an exotherm. Apparently, the shrinkage (collapse of network structure) did not progress linearly, but stepwise. Thereby, the exotherm took the jagged pattern. Conforming to the mechanism, shrunken ceramic body was obtained in the same shape with the original one when a block of the PMMA-forsterite composite was heated above 500 °C.

Because main constituent of the PMMA-forsterite composite was PMMA by mass, its mechanical property was overall close to that of PMMA. Therefore, the composite was machinable, whereas monolithic forsterite xerogel never was. The composite could be obtained as a molded shape. It could be cut and polished into any shape with ease. In Table 1, surface hardness of different solid samples, which was measured by diamond indentation, was compared. Values of modulus of rupture (MOR), which were measured by three-point bending-test, were also given. Monolithic xerogel exhibited very high surface hardness, whereas, it was very low for pristine PMMA. The value of surface hardness for the PMMA-forsterite composite was much closer to that of pristine PMMA. Considering weight fraction of the inorganic moiety was only 8%, this observation suggested that exposed surface of the composite was consisted mostly of PMMA. In three-point bending-test, though, a block of the composite was broken around MOR of 140 MPa. A block of pristine PMMA did not break even at the upper limit of the instrument (>200 Mpa). When it was compared to the variation of the surface hardness (above), mechanical strength as a bulk was weakened in unexpectedly large extent by introduction of very small weight fraction of the inorganic moiety. GPC measurement showed that PMMA had same molecular weight and polydispersity, whether polymerization was carried out in the inorganic networks or in pristine MMA. Therefore, if any prominent change in the mechanical property should occur, it would be caused by the inorganic moiety. Three-point bending-test could not even be carried out on a block of monolithic xerogel, because it was very brittle.
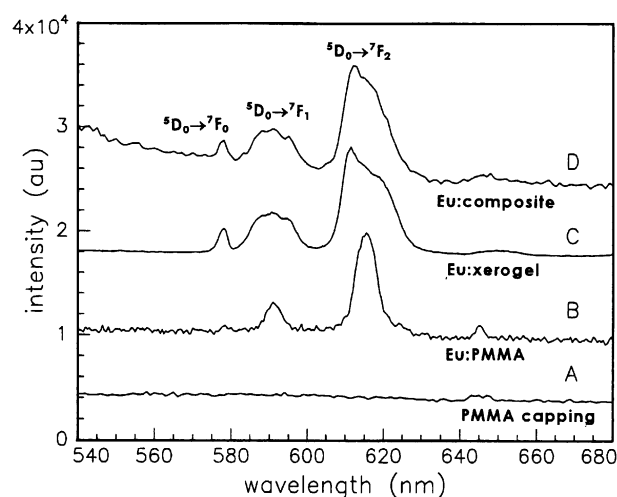
Table 1. Comparison of the mechanical property among forsterite xerogel, pristine PMMA, and the composite of the PMMA-forsterite

	Xerogel Monolith	Pristine PMMA	Composite
Surface Hardness (Kg/mm^2)	33	2.66	5.2
MOR (Mpa)	<1	>200	143

These observations conformed to the morphology of the composite verified in previous sections. Distribution of the brittle inorganic networks throughout PMMA matrix should weaken bulk strength of the composite in such large extent.

Experimental observations, such as high transmittance in visible region, nano-range pore structure, and nano-range texture of the cross-section, indicated that the PMMA-forsterite composite had characteristics as nano-composite. Even though the amount of the inorganic moiety in the composite was very small in terms of its weight, network structure established uniform distribution of the inorganic moiety in the composite. Therefore, it was anticipated that there could be a significant alteration in local environment inside of the composite, in microscopic range.

To attest such alteration of local environment, Eu^{3+} ion was doped into the composite. Because fluorescence from Eu^{3+} was known to be very dependent on local environment, microscopic alteration in local environment of the composite would be detectable. Figure 8 compared the fluorescence spectra from various different samples. In order to see if Eu^{+3} dopant would leach out from the composite, excess MMA was capped on the 'organogel', before initiation of radical polymerization. Spectrum A was taken by using a wafer cut out from the upper part (sole PMMA) of the cylindrical bar. No intensity from Eu^{+3} was observable. This observation indicated that Eu^{+3} dopant, which was doped into the 'organogel', did not leach out into the over-capped MMA. Spectrum B was taken from a wafer cut out from pristine PMMA, which was intentionally doped with Eu^{+3} ions. It was shown that the spectrum was very different from that (spectrum D) taken from a wafer cut out of the PMMA-forsterite composite doped with Eu^{+3} (lower part of the cylindrical bar). Most prominent difference was that $^5D_o \rightarrow$ ^7F_o transition at 578 nm was absent in the spectrum B, which was taken from pristine PMMA doped with Eu^{+3} ions. Also $^5D_o \rightarrow ^7F_1$ transition around 590 nm was observed as a single peak in the pristine PMMA, whereas it was observed as three peaks in the composite. Transition around 612 nm, ^5D_o $\rightarrow ^7F_2$, also exhibited similar difference. The transition at 578nm is observable when site symmetry around Eu^{+3} is low, as in C_s, C_v, or C_{nv}.[27] The peak around 590 nm splits into three when the site symmetry around Eu^{+3} becomes low.[28] Therefore, it was suggested that local environment around Eu^{+3} in the composite had lower symmetry than that in pristine PMMA. Spectrum C was taken from forsterite xerogel doped with Eu^{+3} ions. Resemblance between spectrum C and D is prominent. Site symmetry in forsterite xerogel is considered to be low, because Mg and Si have different coordination numbers (2 and 4) and the network has fractal structure.

Figure 8. Fluorescence spectra taken from PMMA capping over the composite (A), from Eu^{3+} doped in pristine PMMA (B), from Eu^{3+} doped in forsterite xerogel monolith (C), and from Eu^{3+} doped in the composite of the PMMA-forsterite (D).

Therefore, it was suggested that Eu^{+3} ions were exclusively doped into the inorganic moiety of the composite, which provided doping sites in low site symmetry.

Conclusion

By *in-situ* polymerizing MMA inside the inorganic networks of the forsterite 'organogel', organic-inorganic nano-composite of the PMMA-forsterite was synthesized. The forsterite 'organogel' was obtained by exchanging alcohol solvent in the forsterite alcogel directly with MMA. This strategy provided synthetic route to skip over the drying step in the sol-gel processing. Thereby, all those problems related to the drying step, such as shrinkage, cracks, warping, and poor mechanical properties, were bypassed.

The inorganic moiety in the forsterite gel constituted network structure, generating mesopores in size range of 100-400 nm. As MMA was radically polymerized inside the pores, spherical texture of PMMA was resulted. Because nano-property of the inorganic moiety in the forsterite alcogel was preserved, and fixated in the matrix of PMMA, the composite also exhibited properties as a nano-composite. Because heterogeneous domain was sized sub-micron, scattering in UV-vis range was insignificant. Because the inorganic networks were distributed throughout the composite, its mechanical property as a bulk was strongly dependent on the inorganic moiety, even though the surface property was not. The surface property of the composite was strongly related to that of the PMMA moiety.

The PMMA-forsterite composite had amenable property for machining. It could be molded, cut, and polished. Thermal property of the composite was better than pristine PMMA. Depolymerization of PMMA was retarded around 50 °C in the composite. Shrinkage of the inorganic networks during thermal depolymerization of PMMA was apparent.

The composite was doped with Eu^{+3}. Chemical interaction

between the Eu^{+3} ions and the inorganic moiety was fairly strong that the dopant did not leach out during washing. Fluorescence spectrum from Eu^{+3} was altered significantly by introducing only a small weight fraction of the inorganic component to PMMA. The fluorescence spectrum showed that the site symmetry around Eu^{+3} in the composite was lower than that in the pristine PMMA. This observation indicated that ions of Eu^{+3}, which represented a polar inorganic dopant, were doped exclusively to the inorganic moiety in the composite.

References

1. Brinker, C. J.; Scherer, G. W. *Sol-Gel Science-The Physics and Chemistry of Sol-Gel Processing*; Academic press: San Diego, USA, 1990.
2. Park, D. G. *Polymer Science and Technology* **1997**, *8*(3), 248.
3. Wilkes, G. L.; Orler, B.; Huang, H. *Polym. Prepr.* **1985**, *26*, 300.
4. Schmidt, H. *J. Non-Cryst. Solids* **1985**, *73*, 681.
5. Wen, J.; Wilkes, G. L. *Chem. Mater.* **1996**, *8*, 1667.
6. Schubert, U.; Hüsing, N.; Lorenz, A. *Chem. Mater.* **1995**, *7*, 2010.
7. Schmidt, H. *Sol-Gel Optics*; Klein, L. C., Ed.; Kluwer Academic: Boston, 1994; p 451.
8. Landry, C. J. T.; Coltrain, B. K.; Wesson, J. A.; Zumbulyadis, N.; Lippert, J. L. *Polymer* **1992**, *33*(7), 1496.
9. Wung, C. J.; Pang, Y.; Prasad, P. N.; Karasz, F. E. *Polymer* **1991**, *32*(4), 605.
10. Ellsworth, M. W.; Novak, B. M. *Chem. Mater.* **1993**, *5*, 839.
11. Jackson, C. L.; Bauer, B. J.; Nakatani, A. I.; Barnes, J. D. *Chem. Mater.* **1996**, *8*(3), 727.
12. Novak, B. M.; Auerbach, D.; Verrier, C. *Chem. Mater.* **1994**, *6*, 282.
13. Li, X.; King, T. A.; Pallikari-Viras, F. *J. Non-Cystal. Solids* **1994**, *170*, 243.
14. Klein, L. C. *Sol-Gel Optics*; Klein, L. C., Ed.; Kluwer Academic: Boston, 1994; p 215.
15. Kang, J.; Park, S. H.; Kwon, H. Y.; Park, D. G.; Kim, S. S.; Kweon, H. J.; Nam, S. S. *Bull. Korean Chem. Soc.* **1998**, *19*(5), 503.
16. Park, D. G.; Burlitch, J. M.; Geray, R. F.; Dieckmann, R.; Barber, D. B.; Pollock, C. R. *Chem. Mater.* **1993**, *5*, 518.
17. Assink, R. A.; Kay, B. D. *J. Non-Crystalline Solids* **1988**, *99*, 359.
18. Yeager, K. E.; Burlitch, J. M.; Loehr, T. M. *Chem. Mater.* **1993**, *5*, 525.
19. Schaefer, D. W. *MRS Bulletin* **1988**, *8*, 22.
20. Gesser, H. D.; Goswami, P. C. *Chem. Rev.* **1989**, *89*, 765.
21. Kistler, S. S. *J. Phys. Chem.* **1932**, *36*, 52.
22. Lowell, S.; Shields, J. E. *Powder Surface Area and Porosity*, 3rd Ed.; Chapman & Hall: London, UK, 1991; p 11.
23. Gregg, S. J.; Sing, K. S. W. *Adsorption, Surface Area and Porosity*, 2nd Ed.; Academic press: London, UK, 1982; p 111
24. Woignier, T.; Phalippou, J. *J. Non-Crystalline Solids* **1987**, *93*, 17.
25. Beaudry, C. L.; Klein, L. C.; McCauley, R. A. *J. Thermal Analysis* **1996**, *46*, 55.
26. Brinker, C. J.; Scherer, G. W. *Sol-Gel Science-The Physics and Chemistry of Sol-Gel Processing*; Academic press: San Diego, USA, 1990; p 458.
27. Blasse, G.; Bril, A. *Philips Res. Repts.* **1966**, *21*, 368.
28. Blasse, G.; Bril, A. *Philips Technical Review* **1970**, *10*, 304.